IL NUOVO CIMENTO Vol. 28 C, N. 3 Maggio-Giugno 2005
DOI 10.1393/ncc/i2005-10069-5

Unifying XRFs and GRBs with a Fisher-shaped universal jet model(*)

T. Q. Donaghy, C. Graziani and D. Q. Lamb

Department of Astronomy & Astrophysics, University of Chicago
5640 S. Ellis Ave., Chicago, IL, 60615, USA

(ricevuto il 23 Maggio 2005; pubblicato online il 9 Settembre 2005)

Summary. — We show analytically that GRB jets with an emissivity profile given by the Fisher distribution, $\epsilon(\theta) = A \cdot \exp[B \cdot \cos\theta]$, have the unique property of producing equal numbers of bursts per logarithmic interval in $E_{\rm iso}$, and therefore in most burst properties. Since this broad distribution of burst properties is a key feature found by HETE-2, a Fisher-shaped universal jet model can explain many of the observed properties of XRFs, X-ray–rich GRBs, and GRBs reasonably well, in contrast to a power law universal model. For small viewing angles, the Fisher distribution can be approximated by a Gaussian, whose properties have been explored by Zhang B. *et al.* (*ApJ*, **601** (2004) L119). We also show that the Fisher universal jet model produces a broad distribution in the inferred radiated energy $E_\gamma^{\rm inf}$, in contrast to the narrow distribution predicted by the uniform variable-opening-angle jet model (Lamb D. Q. *et al.*, *ApJ*, **620** (2005) 335). Here we present Monte Carlo simulations of both a Fisher-shaped universal jet model and a Fisher-shaped variable-opening-angle jet model.

PACS 98.70.Rz – γ-ray sources; γ-ray bursts.
PACS 01.30.Cc – Conference proceedings.

1. – Introduction

The HETE-2 results show that the properties of XRFs [1], X-ray–rich GRBs, and GRBs form a continuum in the $[S_E(2\text{–}400\ \text{keV}), E_{\rm peak}^{\rm obs}]$ plane [2]. They also show that the relation between the isotropic-equivalent burst energy $E_{\rm iso}$ and the peak energy $E_{\rm peak}$ of the burst spectrum in νF_ν in the rest frame of the burst found by [3] extends to XRFs and X-ray–rich GRBs [4]. A key feature of the distribution of bursts in these two planes is that the density of bursts is roughly constant along these relations, implying equal numbers of bursts per logarithmic interval in S_E, $E_{\rm peak}^{\rm obs}$, $E_{\rm iso}$ and $E_{\rm peak}$. These results, when combined with earlier results [1, 5], strongly suggest that all three kinds of bursts are the same phenomenon. It is this possibility that motivates us to seek a unified jet model of XRFs, X-ray–rich GRBs, and GRBs.

(*) Paper presented at the "4th Workshop on Gamma-Ray Burst in the Afterglow Era", Rome, October 18-22, 2004.

In our previous paper [6], we explored two different phenomenological jet models: a variable jet opening-angle model in which the emissivity is uniform across the surface of the jet and a universal jet model in which the emissivity is a power law function of the angle relative to the jet axis. We showed that while the variable jet opening-angle model can account for the observed properties of all three kinds of bursts, the power law universal jet model cannot easily be extended to account for the observed properties of both XRFs and GRBs. In response to that conclusion, [7,8] considered a quasi-universal Gaussian jet model [9]. They showed that such a model can explain many of the observed properties of XRFs, X-ray–rich GRBs, and GRBs reasonably well.

Here we consider a universal jet model in which the emissivity of the jet as a function of viewing angle is a Fisher distribution (such a distribution is the natural extension of the Gaussian distribution to a sphere). We show that the Fisher distribution has the unique property that it produces equal numbers of bursts per logarithmic interval in $E_{\rm iso}$, and therefore in most burst properties, consistent with the HETE-2 results. We also show that the Fisher universal jet model produces a broad distribution in the inferred radiated energy $E_\gamma^{\rm inf}$. This is not the case for variable-opening-angle jet models because of the extra degree of freedom provided by the distribution of opening angles. Thus we find that the Fisher universal jet model considered here and variable-opening-angle jet model discussed in [6] make different predictions for the distribution in $E_\gamma^{\rm inf}$. Further observations of XRFs can determine this distribution and therefore distinguish between these two models of jet structure. For completeness, we also simulate a variable-opening-angle jet model whose emissivity profile is also a Fisher distribution, and we find similar results to the universal Fisher jet model.

2. – Simulations

The Fisher distribution is the only universal jet profile that satisfies the following two constraints. Let $X_{\rm iso} \equiv \ln E_{\rm iso}$, and $\mu_{\rm v} \equiv \cos\theta_{\rm v}$, where $\theta_{\rm v}$ is the angle between the line-of-sight and the center of the jet. Observations tell us that roughly $\mathrm{d}N/\mathrm{d}X_{\rm iso} = a_1$, where a_1 is some constant. By the definition of $\theta_{\rm v}$ we know that $\mathrm{d}N/\mathrm{d}\mu_{\rm v} = a_2$, where a_2 is another constant. We can describe a universal jet as an arbitrary function of $\mu_{\rm v}$: $X_{\rm iso} = f(\mu_{\rm v})$. We wish to choose $f(\mu_{\rm v})$ so as to satisfy these constraints.

Note that

$$a_2 = \frac{\mathrm{d}N}{\mathrm{d}\mu_{\rm v}} = \frac{\mathrm{d}N}{\mathrm{d}X_{\rm iso}} \cdot \frac{\mathrm{d}X_{\rm iso}}{\mathrm{d}\mu_{\rm v}}, \tag{1}$$

and therefore $\mathrm{d}f/\mathrm{d}\mu_{\rm v} = a_2/a_1$, integrating this expression gives the Fisher distribution

$$E_{\rm iso} = 4\pi A \cdot e^{B\cdot\cos\theta_{\rm v}} = 4\pi\hat{A} \cdot e^{(\cos\theta_{\rm v}-1)/\theta_0^2}, \tag{2}$$

where $B = \theta_0^{-2}$. In the small $\theta_{\rm v}$ limit, this reduces to a Gaussian jet, $E_{\rm iso} = 4\pi\hat{A}\cdot e^{\theta_{\rm v}^2/2\theta_0^2}$.

Integrating the emissivity over the jet gives $E_\gamma^{\rm true}$,

$$E_\gamma^{\rm true} = 2\cdot 2\pi A \int_0^{\pi/2} e^{B\cdot\cos\theta}\, \sin\theta \mathrm{d}\theta = \frac{4\pi A}{B}(e^B - 1). \tag{3}$$

In this work we consider two oppositely directed jets, hence the leading factor of 2. We note that for any non-uniform jet this quantity is *not* the same as the E_γ inferred using the method outlined by [10]. That quantity we term, $E_\gamma^{\rm inf} = E_{\rm iso}\cdot(1-\cos\theta_{\rm j})$, where $\theta_{\rm j} = \max(\theta_0, \theta_{\rm v})$ [7,11]. For $\theta_0 = 0.1$ rad, the quantities $E_{\rm iso}$ and $E_\gamma^{\rm inf}$ vary over

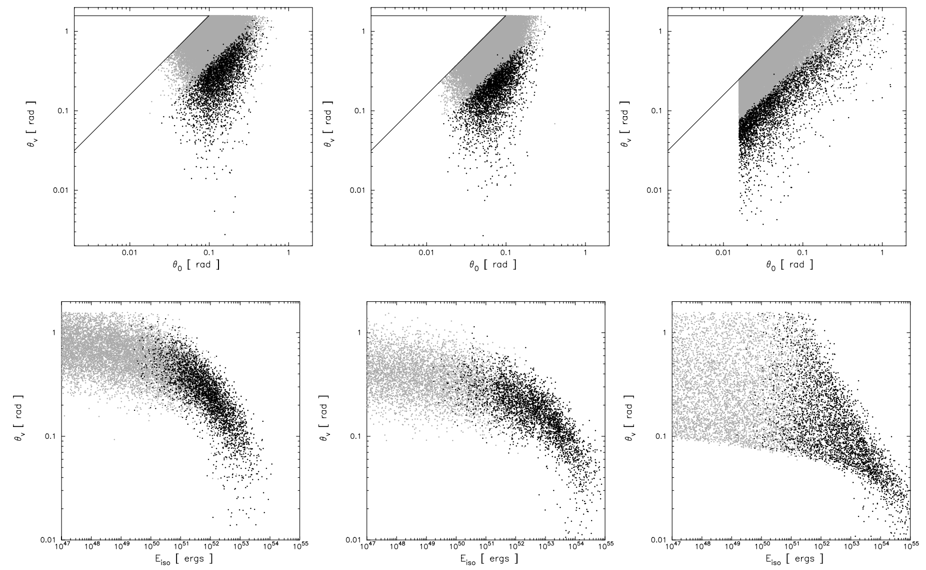

Fig. 1. – Scatter plots of detected (black) and undetected bursts (gray) in the [θ_0, θ_v]-plane (top row) and [E_iso, θ_v]-plane (bottom row) for our 3 models: UFJ1 (left), UFJ2 (middle) and VOAFJ (right). The triangular region in the upper-left corner represents bursts that we do not simulate to increase the percentage of detected bursts in a sample of 50 000.

domains of ~ 43 and ~ 40 decades, respectively, although observational selection effects will truncate both of these distributions. We perform Monte Carlo simulations using the method presented in [6], using the detector thresholds from the WXM on HETE-2.

3. – Results

We consider 3 models. 1) A Universal Fisher Jet model with $\log E_\gamma^\mathrm{true} = 51.1$ and θ_0 values drawn from a log-normal distribution with width 0.2 and $\log \theta_0^0 = -1.0$ (UFJ1), following the parameters of [7,8], 2) a Universal Fisher Jet model with $\log \theta_0^0 = -1.3$ and $\log E_\gamma^\mathrm{true} = 51.8$ (UFJ2), and 3) a Variable Opening-Angle Fisher jet (VOAFJ) model with $\log E_\gamma^\mathrm{true} = 51.5$ and θ_0 values drawn from a power law with index $\alpha_{PL} = -3.3$ and extending for two decades from a maximum of $\pi/2$.

Figures 1 and 2 show the distribution of detected and non-detected bursts in various planes for our 3 models. All 3 models exhibit roughly equal numbers per logarithmic decade in E_iso. For the universal models, this is a natural consequence of the Fisher profile of the jet. For the VOAFJ model this is a consequence of our choice of $\alpha_{PL} = -3.3$. We note that the UFJ1 model is unable to accomodate the highest observed values of E_iso and E_peak. The maximum E_iso generated by a Fisher jet is approximately $E_\mathrm{iso}^\mathrm{max} = E_\gamma^\mathrm{true}/\theta_0^2$, which gives $\sim 1.2 \times 10^{53}$erg for UFJ1 and $\sim 2.5 \times 10^{54}$erg for UFJ2.

The bottom row of fig. 2 shows the histogram of E_γ^inf values for the detected bursts. It is clear that the E_γ^inf distribution does not agree with the inputted E_γ^true distribution. For example, in the UFJ1 model, the peak of the E_γ^true distribution was chosen to correspond to the "standard energy" found by [10, 12], however the model is unable to recover that value using their method. The E_γ^inf distribution typically peaks at a lower energy and has a tail extending to even lower energies. It may be the case that the observed distribution of E_γ^inf values does extend down to lower energies.

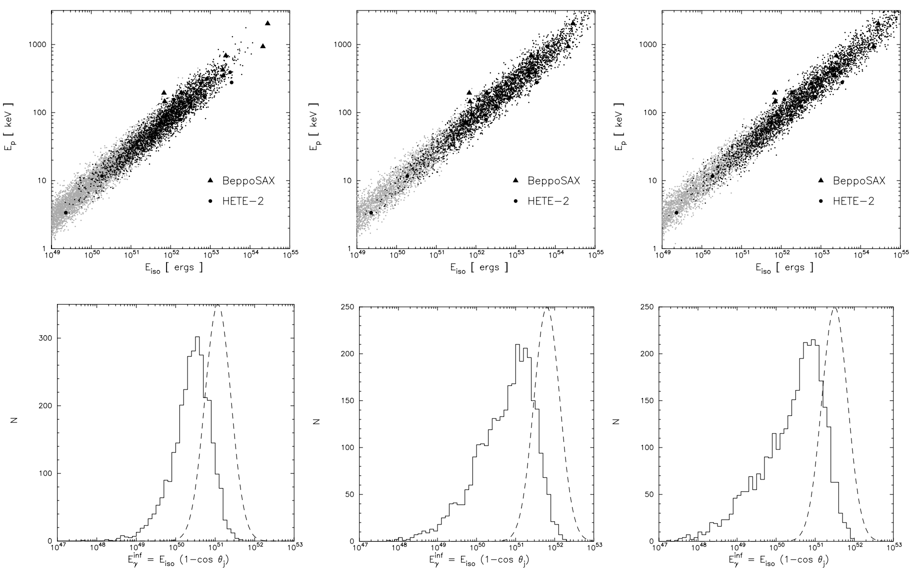

Fig. 2. – Top row shows scatter plots of detected (black) and undetected bursts (gray) in the [$E_{\rm iso}$, $E_{\rm peak}$]-plane for our 3 models: UFJ1 (left), UFJ2 (middle) and VOAFJ (right). Bottom row shows histogram of $E_\gamma^{\rm inf}$ values for detected bursts, as compared to the input distribution of $E_\gamma^{\rm true}$ (dashed curve).

4. – Conclusions

Both universal and variable Fisher jet models can be found that reproduce most of the observed properties of XRFs and GRBs. To accomodate the highest $E_{\rm iso}$ bursts, very small jet opening angles ($\sim 2^\circ - 3^\circ$) may be required in both the variable-opening-angle uniform jet models and in the Fisher models. Finally, $E_\gamma^{\rm inf}$ may be a powerful probe of jet structure, as various models give different predictions for its distribution. More observations of XRFs with redshifts and jet-break times are crucial to answering this question, highlighting the importance of continuing HETE-2 during the *Swift* mission.

REFERENCES

[1] Heise J. *et al.*, in *Proceedings of 2nd Rome Workshop: Gamma-Ray Bursts in the Afterglow Era*, edited by Costa E., Frontera F. and Hjorth J. (Springer-Verlag, Berlin) 2000, p. 16.
[2] Sakamoto T. *et al.*, *ApJ*, **629** (2005) 311 (astro-ph/0409128).
[3] Amati L. *et al.*, *A&A*, **390** (2002) 81.
[4] Lamb D. Q. *et al.*, submitted to *ApJ*, 2005.
[5] Kippen, R. M. *et al.*, 2002, in *Gamma-Ray Burst and Afterglow Astronomy*, edited by Ricker G. R. and Vanderspek R. K., *AIP Conf. Proc.*, **662** (AIP: New York) 2002, p. 244.
[6] Lamb D. Q., Donaghy T. Q. and Graziani C., *ApJ*, **620** (2005) 355.
[7] Dai X. and Zhang B., *ApJ*, **621** (2005) 875 (astro-ph/0407272).
[8] Zhang B., Dai X., Lloyd-Ronning N. M. and Meszaros P., *ApJ*, **601** (2004) L119.
[9] Zhang B. and Meszaros P., *ApJ*, **571** (2002) 876.
[10] Frail D. *et al.*, *ApJ*, **562** (2001) L55.
[11] Kumar P. and Granot J., *ApJ*, **591** (2003) 1075.
[12] Bloom J., Frail D. A. and Kulkarni S. R., *ApJ*, **588** (2003) 945.